Adsorption (2008) 14: 257–263
DOI 10.1007/s10450-007-9095-4

Adsorption properties and photocatalytic activity of TiO_2 and La-doped TiO_2

Minji Jin · Yu Nagaoka · Kazuomi Nishi · Kinuyo Ogawa · Shoji Nagahata · Toshihide Horikawa · Masahiro Katoh · Tahei Tomida · Jun'ichi Hayashi

Received: 30 April 2007 / Revised: 6 October 2007 / Accepted: 20 December 2007 / Published online: 9 January 2008

Abstract Photocatalysts of TiO_2 and La-doped TiO_2 were prepared by calcining the pure TiO_2 sols and the sols mixed with $La(NO_3)_3{\cdot}6H_2O$ at 873 K, respectively. These photocatalysts were characterized by X-ray diffraction (XRD), X-ray photoelectron spectroscopy (XPS), scanning electron microscopy (SEM) and N_2 adsorption-desorption isotherms measurement. As results, the BET surface area, pore diameter, mesopore volume and micropore volume slightly increased, while the crystallite size and the phase structure were little affected by lanthanum doping. The equilibrium adsorption of methylene blue (MB) on the photocatalysts were measured in a dark room. The adsorption isotherms were confirmed to fit to the Langmuir theory. Photocatalytic activities of the photocatalysts were studied by employing the photocatalytic degradation of MB in water and degradation of acetaldehyde in air under UV-irradiation using a black light. Kinetic analysis revealed that the rate controlling steps could be the surface reaction of the adsorbed MB on the catalyst surface for MB degradation and the reaction of adsorbed acetaldehyde with the gaseous acetaldehyde for degradation of acetaldehyde, respectively.

Keywords Adsorption · Photocatalytic activity-TiO_2 · La doping · Methylene blue degradation

M. Jin · Y. Nagaoka · K. Nishi · K. Ogawa · S. Nagahata · T. Horikawa · M. Katoh · T. Tomida (✉)
Institute of Technology and Science, The University of Tokushima, Tokushima, 770-8506, Japan
e-mail: tomida@chem.tokushima-u.ac.jp

J. Hayashi
Department of Chemical Engineering, Kansai University, Osaka, 564-8680, Japan

1 Introduction

Titanium dioxide has been extensively studied due to its high photocatalytic activity which may find potential application for photo-induced removal of harmful organic compounds in air and in water. In recent years, increasing attention has been focused on developing visible-light-active photocatalysts as well as higher active photocatalysts. One method to obtain such photocatalysts is doping with transition metals or other substances (Katoh et al. 2006; Liu et al. 2004; Mozia et al. 2005). Lanthanide ions doping could also improve the activity of TiO_2 photocatalysts. Lanthanide doping was proven to increase the surface area, pore volume, adsorption capacity for organic compounds as well as to suppress electron-hole recombination rates during the process of photocatalytic reaction (Kim et al. 2007; Li et al. 2004, 2005; Liqiang et al. 2004). In addition, it has been reported that lanthanum ions doped in TiO_2 could promote the chemical or physical adsorption of organic compounds on the catalytic surface (Ranjit et al. 1999, 2001a, 2001b). While, the adsorption properties of photocatalysts is strongly concerned in the photocatalytic degradation rate. In some cases, the photocatalytic degradation rate could be expressed by the Langmuir-Hinshelwood equation. However, study on kinetics of photocatalytic degradation using lanthanum doped TiO_2 has been hardly reported.

In the present study, pure and La-doped TiO_2 photocatalysts were prepared, and characterized by X-ray diffraction (XRD), X-ray photoelectron spectroscopy (XPS), UV-vis spectroscopy and N_2 adsorption-desorption isotherms measurement. The adsorption properties of aqueous methylene blue solutions on the catalysts were also investigated in a dark room. Photocatalytic degradation of methylene blue in water and gaseous acetaldehyde in air were carried out by

Table 1 Structural parameters of the photocatalysts prepared

	La:Ti molar ratio	Crystalline size (nm)	BET area (m^2/g)	Pore dia. (nm)	Mesopore volume (cm^3/g)	Micropore volume (cm^3/g)
TiO_2	0 : 100	12.0	46	20.5	0.253	0.017
TiO_2-La-A	8.7 : 91.3	16.0	58	21.4	0.345	0.022
TiO_2-La-B	9.9 : 90.1	12.4	59	21.4	0.339	0.023

UV-irradiation and the kinetics of the photocatalytic decomposition were discussed to evaluate the photocatalytic activity of each photocatalyst.

2 Experimental

2.1 Preparation of TiO_2 and La-doped TiO_2

Titania sol from Institute of Photocatalytic Materials (Aichi, Japan) was used as precursor for preparation of photocatalysts of pure TiO_2 and La-doped TiO_2. The sols mixed with or without dissolved $La(HNO_3)_3{\cdot}6H_2O$ was dried in an oven at 333 K, and calcined at 873 K for one hour under air flow. The lanthanum content in the samples was determined using an Energy Dispersive X-ray fluorescence spectrometer (JSX-3202M, JEOL). These samples are denoted as TiO_2, TiO_2-La-A and TiO_2-La-B (see Table 1).

2.2 Characterization of photocatalyst

X-ray diffraction (XRD) was measured using a Rigaku diffract meter (RINT2500-VHF) with Cu-Kα radiation (100 mA, 30 kV). The surface morphology of the particles was observed using scanning electron microscopy (SEM). The Brunauer-Emmett-Teller (BET) surface area and pore size distribution were determined from N_2 adsorption-desorption isotherms measured by using a Micro pore nitrogen adsorption apparatus (Belsorp, Bel Co. Ltd., Japan). Prior to measurement, the samples were pretreated at 473 K under N_2 flow. XPS measurement was carried out on a Shimadzu ESCA-1000AX using Mg Kα (1253.6 eV) radiation as X-ray source. All the binding energies were reduced to the C 1 s peak at 285.0 eV of the surface adventitious carbon.

2.3 Measurements of adsorption and photocatalytic activity for MB in water

Adsorption isotherms of methylene blue (MB) in water were measured in a dark room thermostated at 298 K. The photocatalyst (0.01 g) was added into 10 cm^3 MB aqueous solution in a quartz tube, and the suspensions were stirred with a roller mixer. At a fixed time intervals, about 4 cm^3 suspensions were collected, then centrifuged, and spectra of the supernatant was measured with an UV-vis spectrophotometer (Shimadzu, UV-2500). The concentration of MB was determined from the absorbance band peak at 664 nm. The adsorbed amount was estimated from the concentration change based on the mass balance.

After establishing adsorption equilibrium, photocatalytic degradation run was started by irradiation with two black-light (Toshiba 4BLB 4W) which were kept about 10 cm above the quartz tube. At a given time interval, the analytical samples were taken from the suspension, and the concentration of MB was determined by the similar method as described above.

2.4 Measurements of photocatalytic activity for gaseous acetaldehyde

The photocatalytic degradation of gaseous acetaldehyde in air was also carried out to evaluate the photocatalytic activity of the samples. The photocatalyst powders were placed on the bottom of a FTIR cell (Volume: ca.116.6 cm^3, Length: 110 mm) equipped with CaF_2 windows (25 mm disks diameter), and then a fixed volume of cold acetaldehyde was injected into the cell. The concentration of acetaldehyde in gas phase increased at the start owing to evaporation, and then decreased gradually until adsorption equilibrium was reached. After that, the photocatalyst was irradiated with the black light through the quartz window mounted on the top of the cell. The gas phase composition in the FTIR cell was analyzed with a FTIR spectrophotometer (Biorad, FTS 3000 MX) at regular time intervals. The concentration of acetaldehyde in gas phase was determined from the peak area at 2733 cm^{-1} of the FTIR spectra.

3 Results and discussion

3.1 Characterization of photocatalyst

Figure 1 shows a typical SEM image of TiO_2-La-B powder. The image shows that the photocatalyst consists of small

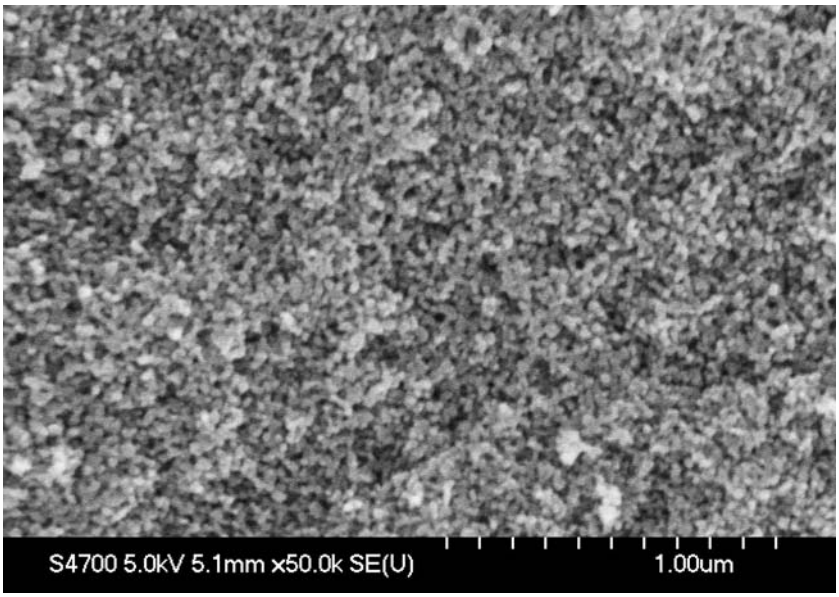

Fig. 1 SEM image of TiO_2-La-B

particles with diameter of 10–20 nm. The similar SEM images were obtained for both powders of TiO_2 and TiO_2-La-A (figures are not shown). From these results, the morphology of the photocatalysts seems not to be modified appreciably by the lanthanum doping.

Figure 2 shows the XRD patterns of TiO_2 and La-doped TiO_2 powders. According to XRD patterns, all samples exhibits anatase and brookite phase of TiO_2. The phase structures were hardly affected by lanthanum doping. In addition to this, the La phase could not observed in the patterns. This indicated that La^{3+} did not enter into TiO_2 crystal lattice to substitute for Ti^{4+}. The XPS spectra of La elements also showed La elements existed in the form of +3 valence in the La-doped TiO_2 (the figure is not shown).

The crystallite size was calculated from X-ray line broadening analysis by the Scherer formula: $D = 0.89\lambda/\beta\cos\theta$, where D is the crystal size in nm, λ is the Cu-Kα wavelength (0.15406 nm), β is the half width of the peak in radian, and θ is the corresponding diffraction angle. The values of crystallite size of TiO_2 and La-doped TiO_2 are in the range of 12–16 nm as shown in Table 1.

To investigate the effects of lanthanum doping on the pore structure and adsorption abilities of the photocatalysts, a set of N_2 adsorption-desorption isotherms measurement was carried out. Figure 3 shows the typical example of the nitrogen adsorption-desorption isotherms of the TiO_2-La-B photocatalyst. The sharp decline in the desorption curve and the hysteresis loop at high relative pressure are indicative of mesoporosity. Pore size distribution of the sample photocatalysts was calculated from the corresponding desorption branch of each isotherm by Dollimore-Heal method and represented in Fig. 4. As seen from the figure, pore size of TiO_2 and La-doped TiO_2 are in the range of 18–25 nm, and La-doped photocatalysts have larger mesopore size than the

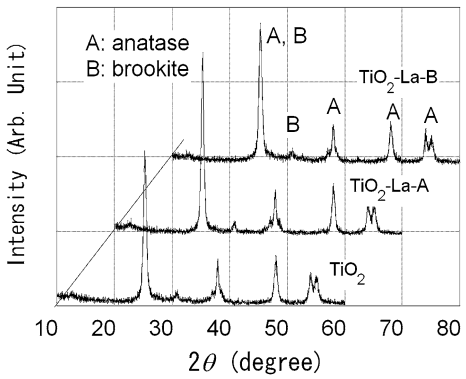

Fig. 2 XRD patterns of TiO_2 and La-doped TiO_2 prepared

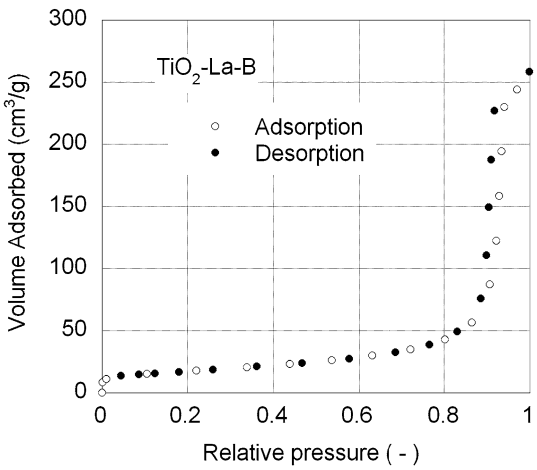

Fig. 3 N_2 adsorption-desorption isotherms of different photocatalysts

pure TiO_2 photocatalyst. Other structural parameters such as specific surface area (S_{BET}) and mesopore volume were

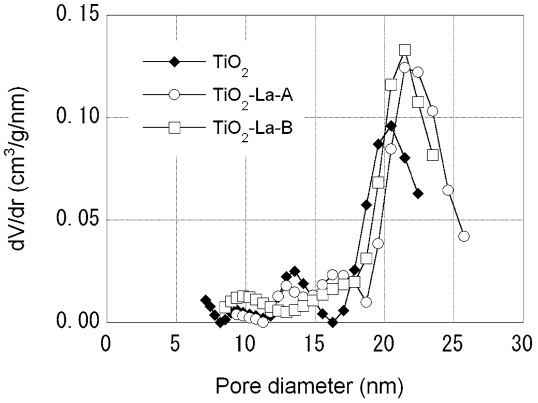

Fig. 4 Pore size distributions for the different photocatalysts

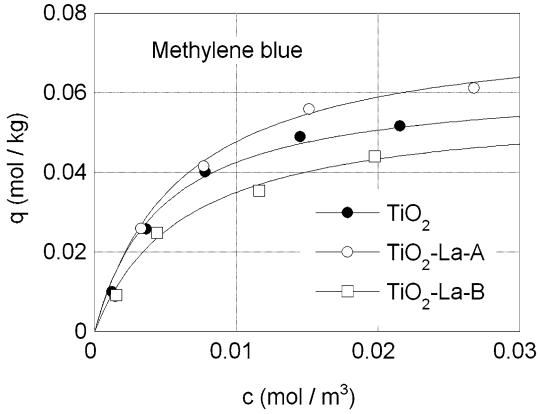

Fig. 5 Adsorption isotherms of MB on different photocatalysts

Table 2 Langmuir parameters for adsorption of aqueous methylene blue on the samples

	q_0 (mol/kg)	K (m^3/mol)
TiO_2	0.063	213
TiO_2-La-A	0.077	163
TiO_2-La-B	0.057	159

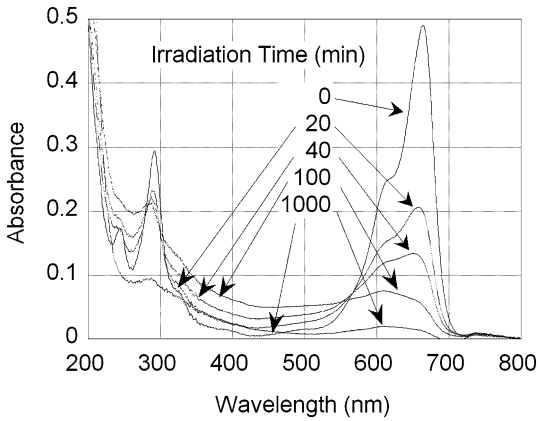

Fig. 6 UV-vis spectra of MB solutions at different irradiation times using TiO_2-La-A photocatalyst

also calculated on the basis of N_2 adsorption-desorption isotherms. These are summarized in Table 1. The BET surface area, mesopore diameter, micropore volume and mesopore volume were increased owing to the lanthanum doping.

3.2 Adsorption isotherms of methylene blue in water

Figure 5 indicates the adsorption isotherm plots of MB onto the different photocatalysts. Symbols represent experimental data and solid lines are the calculated values by the Langmuir equation using the parameters shown in Table 2, which were determined by the conventional Langmuir plots based on the following Langmuir equation:

$$q = q_0 K c/(1 + K c), \tag{1}$$

where q_0 and K are the adsorption capacity and the equilibrium constant, respectively. As seen from the figure, the adsorption isotherms are well represented by the Langmuir model.

3.3 Photocatalytic degradation of methylene blue in water

Photocatalytic activities of the catalysts were examined by employing the photocatalytic degradation of MB in water under UV-irradiation with the black light. Figure 6 represents the variation in the absorption spectra of MB owing to photocatalytic degradation in the presence of the photocatalyst powders of TiO_2-La-A. As seen from the figure, absorbance at 664 nm decreased with increasing the irradiation time due to the photocatalytic degradation of MB. While, the absorbance peaks in the range of 300–560 nm increased, after then gradually decreased until the solution became colorless. This indicates the formation of intermediate products by photocatalytic degradation of MB.

3.4 Degradation rate of methylene blue

The time courses of MB concentration change owing to photocatalytic degradation using TiO_2-La-A are shown in Fig. 7. As can be seen, the concentration decreased steeply in initial period, and then gradually decreased with increasing irradiation time. Similar results were also obtained for the TiO_2 and TiO_2-La-B (They are not shown). In general, initial reaction rate, r_0, is defined by the (2). In this study, the initial degradation rate was estimated from the average concentration decline for 20 minutes after starting irradiation.

$$r_0 = -\left(\frac{dc}{dt}\right)_{t\to 0}. \tag{2}$$

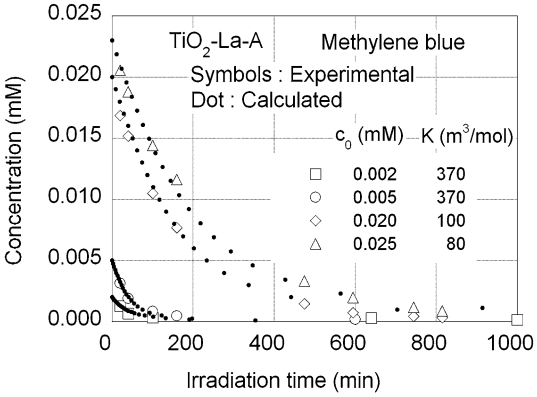

Fig. 7 Photocatalytic degradation of MB at different initial concentration: *dotted lines*, calculated from (4) using $k = 2.47 \times 10^{-4}$ m^3/kg/min and K values in the figure

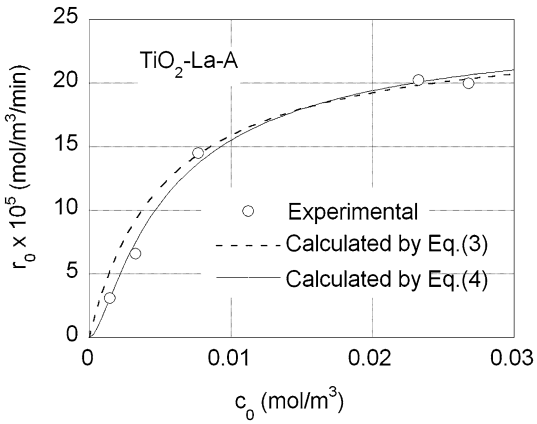

Fig. 8 Relation between the initial degradation rate and initial concentration

Figure 8 represents the relation between the initial degradation rate and initial concentration, c_0, for photocatalytic degradation of MB using TiO_2-La-A. As seen from the figure, r_0 increased sharply in lower concentration region and then became to plateau. This is a typical behavior of Langmuir-Hinshelwood kinetics which is expressed as follows:

$$r_0 = \frac{\alpha k_1 K c_0}{1 + K c_0}, \tag{3}$$

where k_1 and K are the reaction rate constant and the adsorption equilibrium constant, respectively. α is the ratio of the weight of photocatalyst to the solution volume used. However, it is clearly seen that the calculated values did not coincide satisfactorily with the experimental data in the lower concentration range. While, the experimental data of r_0 were thoroughly represented by the following equation:

$$r_0 = \alpha k_1 \left(\frac{K c_0}{1 + K c_0} \right)^2. \tag{4}$$

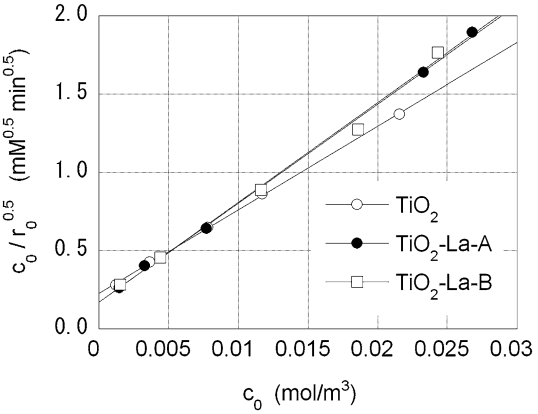

Fig. 9 Correlations of the initial reaction rate for photocatalytic degradation of aqueous MB solutions

Table 3 Parameters in (4)

	K (m^3/mol)	k_1 (mol/kg/min)
TiO_2	236	3.50×10^{-4}
TiO_2-La-A	370	2.47×10^{-4}
TiO_2-La-B	372	2.50×10^{-4}

This equation means that the rate controlling step is the surface reaction of the adsorbed MB.

Figure 9 shows the plots of $c_0/r_0^{0.5}$ against c_0 based on (4). As seen from the figure, good linear relations were obtained in the whole range of the initial concentration irrespective of the photocatalyst used. The values of k_1 and K were determined from the slope and the intercept of each line, and listed in Table 3. As results, k_1 value decreased, while K value increased owing to the lanthanum doping.

The time course of concentration change owing to photocatalytic degradation could be estimated from (2) and (4). In Fig. 7, the calculated time courses were compared with experimental ones. In this calculation, the values of k_1 and K in Table 3 were used except for K values of 100 and 80 m^3/mol shown in the figure. The results show that the calculated value is in good agreement with the experimental value. This justification implies that the decomposition rate could be expressed by (4).

3.5 Degradation rate of gaseous acetaldehyde in air

Composition of gas phase owing to photocatalytic degradation of acetaldehyde in air was monitored using FTIR. Figure 10 shows the typical FTIR spectra of the gas-phase in the FTIR cell at different irradiation times. The bands at 2733 and 1735 cm^{-1} assigned to acetaldehyde decreased with an increase in irradiation time. While the bands at 2361 and 2340 cm^{-1} attributed to CO_2 increased, and the bands at

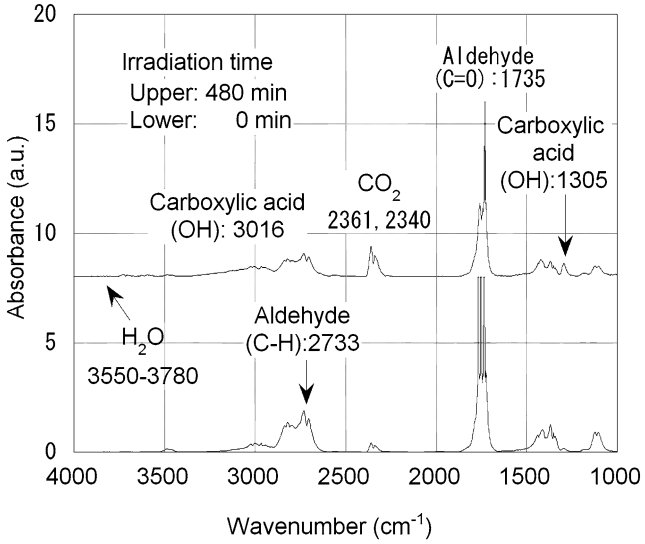

Fig. 10 FTIR spectra of gas phase in the cell at different irradiation times

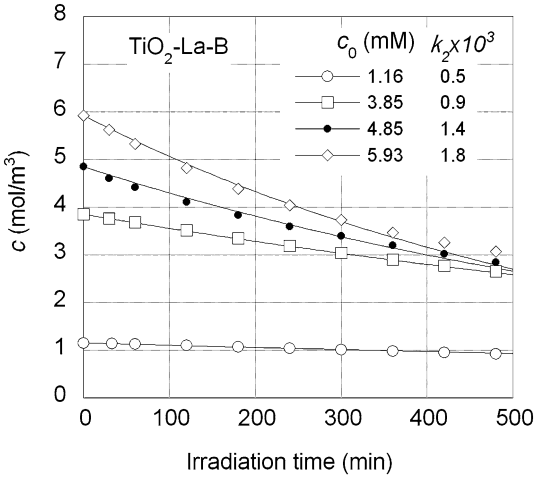

Fig. 11 Time courses of concentration change of acetaldehyde by photocatalytic degradation: *lines*, calculated from (5) using k_2 values shown in the figure

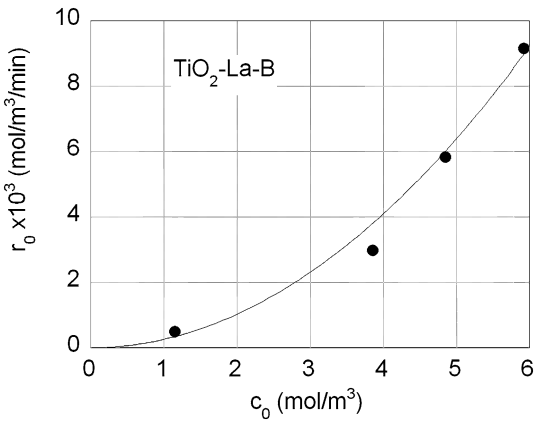

Fig. 12 Relation between the initial degradation rate and the initial concentration

3550–3780 cm^{-1} assigned to H_2O and the small peaks at 1305 and 3016 cm^{-1} assigned to carboxyl acid appeared in the spectra. The FTIR spectra revealed that acetaldehyde was decomposed mainly to CO_2, H_2O and minor unidentified intermediates of carboxylic acid.

Figure 11 illustrates the time courses of the concentration change of acetaldehyde owing to the photocatalytic degradation by TiO_2-La-B. As seen from the figure, the initial decline increased with an increase in initial concentration. The individual time course was approximately expressed by the pseudo-first-order reaction as expressed by the following equation:

$$\ell n(c/c_0) = -\alpha k_2 t. \tag{5}$$

The lines in the figure were calculated values from (5) using the values of k_2 shown in the figure, which were determined by fitting the calculated curves to the experimental ones. However, k_2 values tend to increase with an increase in initial concentration.

The relation between the initial reaction rate and initial concentration for photocatalytic degradation of gaseous acetaldehyde by TiO_2-La-B are shown in Fig. 12. Different from the photocatalytic degradation of MB in water, the initial degradation rate of acetaldehyde could be expressed by the following equation:

$$r_0 = \frac{\alpha k_2 K c_0^2}{1 + K c_0}. \tag{6}$$

This means that the rate controlling step of photocatalytic degradation of acetaldehyde is possibly the reaction of acetaldehyde in air with the adsorbed acetaldehyde on the photocatalyst surface.

4 Conclusions

Photocatalysts of TiO_2 and La-doped TiO_2 were prepared, and characterized by X-ray diffraction (XRD), X-ray photoelectron spectroscopy (XPS), UV-spectroscopy and N_2 adsorption-desorption isotherms measurement. It was shown that the mesopore diameter, specific surface area and mesopore volume increased, while crystalline size and surface morphology were not influenced by the lanthanum doping. Photocatalytic activities of the samples were examined by employing the photocatalytic degradation of methylene blue in water and degradation of gaseous acetaldehyde in air under UV-irradiation with black lights. Kinetic analysis revealed that the rate controlling steps were the surface reaction of the adsorbed methylene blue for degradation of methylene blue in water and the reaction of adsorbed acetaldehyde with the gaseous acetaldehyde for degradation of acetaldehyde in air, respectively.

Nomenclature

- c Concentration of species, mol/m^3
- c_0 Initial concentration, mol/m^3
- k_1 Reaction rate constant in (3) or (4), mol/kg/min
- k_2 Reaction rate constant in (5) or (6), m^3/kg/min
- K Adsorption equilibrium constant, m^3/mol
- q Amount of adsorbed, mol/kg
- q_0 Adsorption capacity, mol/kg
- r_0 Initial reaction rate, mol/m^3/min
- t Run time, min
- α Parameter defined by the following: catalyst weight/volume, kg/m^3

References

Katoh, M., Aihara, H., Horikawa, T., Tomida, T.: Spectroscopic study for photocatalytic decomposition of organic compounds on titanium dioxide containing sulfur under visible light irradiation. J. Colloid Interface Sci. **298**, 805–809 (2006)

Kim, H.R., Lee, T.G., Shul, Y.G.: Photoluminescence of La/Ti mixed oxide prepared using sol-gel process and their pCBA photodecomposition. J. Photochem. Photobiol. A: Chem. **185**, 156–160 (2007)

Li, F.B., Li, X.Z., Hou, M.F.: Photocatalytic degradation of 2-mercaptobenzothiazole in aqueous La^{3+}–TiO_2 suspension for odor control. Appl. Catal. B: Environ. **48**, 185–194 (2004)

Li, F.B., Li, X.Z., Ao, C.H., Lee, S.C., Hou, M.F.: Enhanced photocatalytic degradation of VOCs using Ln^{3+}–TiO_2 catalysts for indoor air purification. Chemosphere **59**, 787–800 (2005)

Liqiang, J., Xiaojun, S., Baifu, X., Baiqi, W., Weimin, C., Honggang, F.: The preparation and characterization of La doped TiO_2 nanoparticles and their photocatalytic activity. J. Solid Chem. **177**, 3375–3382 (2004)

Liu, G., Zhang, X., Xu, Y., Niu, X., Zheng, Li., Ding, X.: Effect of $ZnFe_2O_4$ doping on the photocatalytic activity of TiO_2. Chemosphere **55**, 1287–1291 (2004)

Mozia, S., Tomaszewska, M., Kosowska, B., Grzmil, B., Morawski, A.W., Kalucki, K.: Decomposition of nonionic surfactant on a nitrogen-doped photocatalyst under visible-light irradiation. Appl. Catal. B: Environ. **55**, 195–200 (2005)

Ranjit, K.T., Cohen, H., Willner, I., Bossmann, S., Braun, A.M.: Lanthanide oxide-doped titanium dioxide: Effective photocatalysts for the degradation of organic pollutants. J. Mater. Sci. **34**, 5273–5280 (1999)

Ranjit, K.T., Willner, I., Bossmann, S.H., Braun, A.M.: Lanthanide oxide doped titanium dioxide photocatalysts: Effective photocatalysts for the enhanced degradation of salicylic acid and *t*-cinnamic acid. J. Catal. **204**, 305–313 (2001a)

Ranjit, K.T., Willner, I., Bossmann, S.H., Braun, A.M.: Lanthanide oxide-doped titanium dioxide photocatalysts: Novel photocatalysts for the enhanced degradation of *p*-chlorophenoxyacetic acid. Environ. Sci. Technol. **35**, 1544–1549 (2001b)